# Sonomyography: Monitoring Morphological Changes of Forearm Muscles in Actions with the Feasibility for the Control of Powered Prosthesis

YP Zheng, MMF Chan, J Shi, X Chen, and QH Huang

Department of Health Technology and Informatics, The Hong Kong Polytechnic University, Kowloon, Hong Kong SAR, China

**Keywords**: ultrasound, sonomyography, SMG, muscle, prosthesis control, motion analysis, electromyography, EMG

Corresponding Author:
Yongping Zheng, PhD.
Department of Health Technology and Informatics,
The Hong Kong Polytechnic University,
Hung Hom, Kowloon, Hong Kong SAR, P.R.China
Tel: 852-27667664
Fax: 852-23624365
Email: ypzheng@ieee.org

Submitted to: **Medical Engineering and Physics**
First Submission: **Dec 30 2004**
1st revision: **Jun 20 2005**
2nd revision: **Jul 9 2005**

**ABSTRACT**

Electromyography (EMG) has been widely used for the assessment of musculoskeletal functions and the control of electrical prostheses, which make use of the EMG signal generated by the contraction of the residual muscles. In spite of the successful applications of EMG in different fields, it has some inherent limitations, such as the difficulty to differentiate the actions of neighboring muscles and to collect signals from deep muscles using the surface EMG. The majority of current EMG controlled prostheses can only provide sequential on-off controls using signals from two groups of muscles, so the users are required to put many conscious efforts in monitoring the speed and range of motion of the terminal devices being controlled. Recently, many alternative signals based on the detection of dimensional changes of muscles or tendons during actions have been reported. The objective of this study was to investigate the potential of the dimensional change of muscles detected using sonography for musculoskeletal assessment and control. A portable B-mode ultrasound scanner was used to collect the dynamic ultrasound images of the forearm muscles of six normally-limbed young adults and three amputee subjects. A motion analysis system was used to collect the movement of the wrist angle during the experiments for the normal subjects. It was demonstrated that the morphological changes of forearm muscles during actions can be successfully detected by ultrasound and linearly correlated ($R^2$ = 0.876±0.042, mean±SD) with the wrist angle. We named these sonographically detected signals about the architectural change of the muscle as sonomyography (SMG). The mean ratio between the wrist angle and the percentage deformation of the forearm muscle was 7.2±3.7 deg/% for the normal subjects. The intraclass correlation coefficient (ICC) of this ratio among the three repeated tests was 0.868. The SMG signals from the residual forearms were also successfully detected when

the three amputee subjects contracted their residual muscles. The results demonstrated that SMG had potentials for the musculoskeletal control and assessment.

## 1. Introduction

There are a number of existing techniques for tracking the human posture and movement. An external reference source like magnetic wave, ultrasound, or light can be configured to detect the motion of a body part. A body part can also be used as a reference to detect the motion of another part using devices like flex sensors. Other techniques for sensing human posture and movement include: gyroscope and accelerometer for detecting dynamic motion, inclinometer for posture detection, data gloves and jackets for gesture and posture detection. The movement of body parts can also be detected using the information generated inside the body, such as electromyography (EMG) signals taken with electrodes on the skin surface or inserted into the muscle, tendon movement sensed with pneumatic sensor on the skin surface, dimensional change of the soft tissues sensed by Hall sensors, and signals obtained from the neural motor cortex, etc.

Using prosthesis as an example, the majority of upper limb powered prosthetic devices are controlled by surface EMG signals generated by muscle activities since the invention of myoelectric prostheses in 1950s [1]. However, some inherent limitations of myoelectric control have not been overcome yet [2]. For example, many conscious efforts are still required to control the myoelectric prostheses [3]. Another limitation is that most commercial myoelectric prostheses can provide only one practical degree of freedom

(DOF), directed by the flexion-extension of arm muscles [4]. Intensive research efforts have been ongoing to extract more independent channels of control signals from EMG with advanced signal processing techniques including time-frequency analysis, wavelet analysis, neural network, fuzzy classification, etc. [5-8]. In addition to the decoding of EMG signals, many recent efforts have also been made on the decoding of the electroencephalography (EEG) signals [9] or the volitional signals from the original motoneuron pathways [10-12]. Currently, surface EEG collected non-invasively can only provide relatively low information rate. The invasive approach using neurochip implants may finally provide a comprehensive human-machine connection, particularly for patients with spinal cord injury, though most of the current researches are still on animal models. EMG signals are normally preferred if they can be collected and decoded for corresponding control, as the use of the muscles can prevent atrophy [13,14]. In addition to EMG, the acoustic signals generated from muscles during contraction have also been investigated for control purposes [15-18]. It has been reported that the myoacoustic signal appeared sensitive to external noises.

Many alternative approaches have been investigated for sensing the motion of the residual limb muscles in the upper-limb prosthetic control. It has been reported to use the mechanical force provided by a tunnel muscle or tendon (generated using tunnel cineplasty) to control a powered prosthesis [18,20]. Tunnel cineplasty is a technique for attaching muscle in the residual limb to the prosthesis. Since the force sensation of the muscle can be maintained in the approach using the tunnel muscle, the subject can have a physiological feedback in controlling the prosthesis. As a cost, this approach requires additional surgeries. Early in 1951, a prosthesis was developed using mechanical amplification of muscle section dimension as a control interface [21]. Different transducers have been used to detect the

surface contour change for prosthetic control [3,22] or monitor muscle states during functional electrical stimulation [23]. Another research group developed a system based on pneumatic sensors to detect residual tendon motions for the control of multi-finger prostheses [24,25]. It was demonstrated that the force between the skin surface and prosthetic socket generated by the residual tendon movement could be used for the proportional control of prostheses [26]. These techniques used morphological changes of residual limb tissues which were detected on the skin surface only.

Ultrasound imaging has been widely used for the dynamic assessment of the heart tissues and blood vessels. Musculoskeletal ultrasound tissue assessment is normally focused on static or quasi-static examination of muscles, tendons and other tissues [27]. Recently, the restriction to median nerve movement has been observed in cross-sectional images for carpal tunnel syndrome [28,29]. Many researchers have developed various approaches to measure tissue translations, rotations and deformations in 2-dimensional (2D) and 3-dimensional (3D) spaces for different musculoskeletal tissues [30-34]. Dynamic assessments of tissue deformation using ultrasound have also been used for elastography, where an external static load or vibration is applied on the tissue [35,36]. National Aeronautics and Space Administration (NASA) in the United States developed an apparatus using an ultrasonic transmission method to monitor the overall volume changes of human limbs in zero gravity in the space [37]. Another technique was reported to monitor the trunk alignment by measuring the distance of two ultrasound transducers attached on the skin surface with the ultrasound signals passing along the skin layer [38]. Ultrasound imaging has also been used to assess the movement of deep muscles during physiotherapy activities [39] and the residual bone movement inside a residual limb confined within a prosthetic

socket during gait [40]. Simultaneous measurement of EMG and ultrasound signals have also been reported for recording activities of muscles in a quasi-static way [41], for monitoring the activities of respiratory muscles [42], and for measuring nerve-conduction velocity associated with electrical stimulation [43]. In these studies, the morphological changes of muscles and other tissues measured using ultrasound during various motions are traditionally used for diagnosis or assessment, but not targeting for control purposes.

In the present study, ultrasound imaging was used to detect the morphological changes of muscles or other tissues during actions, named as sonomyography (SMG). The sonomyographic signals could be potentially used for the control of prosthesis. Based on the capability of ultrasound to detect morphological changes of underlying soft tissues at different depths and different locations, the movements of the individual muscles and tendons can be obtained. Six normal subjects and three amputee subjects were tested on the forearms and their results were reported. For the normal subjects, the SMG signal was correlated with the wrist angle captured by a motion analysis system. The potential application of SMG signal for the prosthesis control is discussed.

## 2. Methods

### *2.1.Experimental Setups*

In this study, sonographs of wrist extensor muscles were recorded using a B-mode ultrasound scanner (180 Plus, SonoSite SonoSite, Inc., Bothell, WA, USA) with a 10-5 MHz 38mm transducer (L38, SonoSite). The sonographs were digitized and input to a computer using a USB video capture device (PCTV, Pinnacle, Singapore) at a rate of 30

frames per second. The wrist motions were captured by a motion analysis system (Vicon 370 version 2.6, Vicon Motion Systems Ltd., Oxford, UK) through four synchronized infrared cameras (with a sampling rate of 120 Hz) which detected lightweight, spherical (4mm diameter) reflective markers. Two modified computer mice connected with a single switch were used to initiate simultaneous data acquisition from both the PCTV and Vicon systems. The block diagram of the experimental setup is shown in *Figure 1*. A camera tripod was modified to hold the ultrasound probe in a desired orientation and location above the forearm to be tested. The time delay between the two data collection system was calibrated using a method similar to that described in the development of a 3D ultrasound imaging [44]. A reflective marker was attached on the ultrasound probe. When the probe was moved cyclically up and down inside a water tank, its displacement was detected from both the acquired ultrasound images and the Vicon motion data. The time delay between the data set was then calculated using a cross-correlation algorithm as follow:

$$R_{xy}[m] = \frac{\sum_{i=0}^{N-1}(x(i)-\bar{X})(y(i+m)-\bar{Y})}{\sqrt{\sum_{j=0}^{N-1}(x(j)-\bar{X})^2\sum_{k=0}^{N-1}(y(k+m)-\bar{Y})^2}} \quad (1)$$

where *x(i)* and *y(i)* are the data sequences of the displacements measured by the two methods; $N$ is the length of the sequence; $\bar{X}$ and $\bar{Y}$ are the means of *x(i)* and *y(i)*, respectively. By changing $m$, one sequence can be shifted in relation to the other sequence and the cross-correlation coefficients $R_{xy}$ for each $m$ can be calculated. The $m$ corresponding to the maximum $R_{xy}$ represents the shift required to make the two sequences overlap with each other. Knowing the sampling rate of the sequence, the time delay can then be calculated from the shift.

*2.2. Experiment on Normal Subjects*

Six healthy volunteers with ages ranging from 22 to 28 years old were recruited in this study. Their dominant hands were selected for the investigation. The subjects were seated in a comfortable chair with their forearms under study rest on the table and centered in the calibrated 3D space. They were asked to perform wrist extension and flexion repeatedly, guided by the audio beat of a metronome (30 beats per minutes). The wrist movements and the ultrasound images of the muscle were recorded simultaneously. Three separate trials were assigned to each subject with a rest of approximately 2 min between two adjacent trials. The subject was asked to perform three cycles of wrist flexion-extension in each trial. Reflective markers were stacked at the 3$^{rd}$ metacarpal head, medial and lateral styloid processes, and 2/5 of the forearm length between the radius and ulna (*Figure 2*). The cameras emitted infrared beams and sensed the reflection from the markers. Their motions were then captured and the corresponding 3D coordinations were recorded. The motion data were then extracted with the software provided with the Vicon motion analysis system and exported for further analysis in Excel (Microsoft, US).

The synchronized ultrasound images were recorded and processed by a program written in Visual C++ (*Figure 3*) to perform muscle boundaries tracking. The program provided up to five rectangular blocks for the selection of regions of interest. The ultrasound images were imported to the program interface and displayed and analyzed frame by frame. In this study, two rectangular blocks were used to track the upper and lower boundaries of the extensor carpi radialis shown in the ultrasound images (*Figure 4*). The blocks followed the movements of muscle boundaries during the playback of the ultrasound images based on a 2D cross-correlation tracking algorithm as follow:

$$R_{xy}(m,n) = \frac{\sum_{i=0}^{I-1}\sum_{j=0}^{J-1}[x(i,j)-\bar{X}][y(i+m,j+n)-\bar{Y}]}{\sqrt{\sum_{i=0}^{I-1}\sum_{j=0}^{J-1}[x(i,j)-\bar{X}]^2 \sum_{i=0}^{I-1}\sum_{j=0}^{J-1}[y(i+m,j+n)-\bar{Y}]^2}} \quad (2)$$

where *x(i,j)* and *y(i,j)* are the pixels in the selected image blocks of two continuous frames. *I* and *J* represent the 2D dimension of the selected image block in pixel; $\overline{X}$ and $\overline{Y}$ are the means of *x(i,j)* and *y(i,j)*, respectively. By changing *m* and *n*, one image block can be shifted in 2D in relation to the other and the cross-correlation coefficients $R_{xy}$ for each *m* and *n* can be calculated. The *m* and *n* corresponding to the maximum $R_{xy}$ represent the 2D shifts required to make the two image blocks overlap with each other. Knowing the distance between two adjacent pixels, the displacement of the selected image in 2D can then be calculated from the pixel shift. The net displacement between the centres of the two blocks, which represented the muscle deformation, was then calculated for each frame of the ultrasound images.

### *2.3. Experiment on the Amputee Subject*

In this feasibility study, three amputee subjects were recruited to validate that the experimental protocol could be extended to limb-deficient individuals. The residual limbs should have no substantial scar tissue that may provoke the co-contraction of muscles. As shown in the demographic information (Table 1), one subject was using a powered prosthesis with myoelectrical control and the other two using body-powered prostheses. The subject was seated on a comfortable chair with his residual limb placed on the table, and asked to intend extending his phantom wrist guided by the audio beats from a metronome (30 beats per minute). Meanwhile, the ultrasound images of the residual limb

were recorded over the extensor muscle group using the ultrasound probe (*Figure 5*). Three separated trials were performed by the amputee subject with a rest of approximately 2 min between two adjacent trials. The subject was asked to perform three cycles of wrist flexion-extension in each trial.

## 3. Results

### *3.1.Results of normal subjects*

Totally fifty-four data sets were successfully obtained for the six normal subjects. Four parameters were derived from each data set including: the range of motion of the wrist joint, the initial muscle thickness, the maximum muscle deformation, and the ratio of the wrist extension angle and the percentage muscle deformation. According to the measured data, the cycle duration was 2.6 ± 0.3 seconds (ranging from 2.0 to 3.0 seconds), which was slightly longer than the intended duration (2.0 seconds) possibly due to the response time required. The variation might be due to the difference in subjects' reaction to the audio beat that guided them to perform the wrist flexion-extension. The initial muscle thickness was 17.9 ± 0.8 mm (ranging from 15.3 to 22.3 mm). The maximum muscle deformation was 14.3 ± 6.0% (ranging from 4.2% to 15.5 %). The maximum range of motion of the wrist flexion-extension was 44.2° ± 6.2° (ranging from 34.9° to 50.9°).

*Figure 6* illustrates a typical data set of the transient wrist extension angle and the percentage muscle deformation. The right Y axis indicates the muscle deformation in percentage while the left Y axis indicates the wrist flexion-extension angle in degrees. The X axis indicates the measurement time in seconds. Results of all the subjects showed

similar patterns. The overall trend was that the wrist extension angle was closely correlated with the muscle deformation (*Figure 6*).

The relationship between the wrist flexion-extension angle and the corresponding muscle deformation was further studied using their ratio, i.e. the slopes of the linear regression between the wrist flexion-extension angles and the percentage muscle deformations (*Figure 7*). Results of all the subjects showed similar trends and the overall mean $R^2$ value for the linear regression was 0.875 ± 0.042. *Figure 8* shows the ratio between the wrist extension angle and the percentage muscle deformation for the six subjects. The overall mean value of the angle-deformation ratio was 7.2 ± 3.7 deg/% (ranged from 1.2 ± 0.2 to 12.4 ± 3.2 deg/%). A two-factor ANOVA demonstrated that the ratios were significantly ($p=0.0003$) different among the subjects but not ($p=0.2$) among the three repeated tests for each subject. The intraclass correlation coefficient (ICC) for the three repeated tests was 0.868, which was calculated using SPSS (SPSS Inc., Chicago, IL, USA).

*3.2. Preliminary Results of the Amputee*

A typical ultrasound image obtained from the residual forearm of the amputee subject is shown in *Figure 9a*. It was found that the muscle regions and their boundaries could be identified on the image, though they were less clear in comparison with those of the normal subjects as shown in *Figure 4*. When the residual muscle was contracted, its dimensional change could be clearly observed. *Figure 9b* illustrates a typical data set of the transient percentage muscle deformation versus the measurement time. Results of the other two trials showed similar patterns. Figures 10 and 11 show the typical results obtained from the

other two amputee subjects, who were using body-powered prostheses. It could be noted that similar transient muscle deformations were obtained, though the amputations had been done for over 20 years for these two subjects. The preliminary results demonstrated that the SMG signal could be successfully collected from the amputee residual forearm muscles and had potentials for the prosthesis control. It was also noted that the curve of the transient muscle deformation of the amputee was not so smooth in comparison with those of the normal subjects.

## 4. **Discussion**

In this study, we introduced a new signal related to the morphological change of the muscle during its contraction. This signal, named as sonomyography or SMG, was extracted from the real-time ultrasound images and could be potentially used for the control of powered prosthesis and the dynamic assessment of musculoskeletal functions. It has been proposed that using control signals based on the hand and finger actuators that remained intact in the residual limb would require less conscious effort in the prosthesis control [24]. These actuator tissues include the extrinsic muscles and tendons controlling the flexion-extension of the wrist and metacarpophalangeal joints. The dimensional change of these tissues is originally correlated to the motion of the related joint. Therefore, the signal related to this dimensional change can be used to control the terminal devices being used by the amputee. The use of this kind of control signal would encourage the amputee subject to control the prosthesis without the conscious efforts so that it may benefit the users with functional improvements.

The present study demonstrated that there was a good linear relationship between the wrist extension angle and the corresponding extensor in the normal adult young subjects (n=6), so a relatively simple control algorithm could be used. Whether such a linear relationship also exists for other joints and their corresponding muscles requires further experimental support. Since amputee subjects can feel the contraction level of their residual muscles, which in turn is related to the wrist extension, they may be able to partially sense without consciousness the open-close level or other status of the powered prosthesis if it is controlled by SMG proportionally. Such a feature is difficult to achieve using the currently available EMG control approach. The preliminary results obtained from three amputee subjects in the present study demonstrated that the SMG signal could be successfully obtained from the residual forearm muscles and the SMG magnitude was in a similar range as those collected from the normal subjects. One amputee subject was using a powered prosthesis with myoelectrical control and the other two using body-powered prostheses. It was generally believed that the atrophy of the residual muscles of the powered prosthesis user should be less serious in comparison with those using body-powered prosthesis. It appeared in this study that the subject using powered prosthesis did not demonstrate a stronger SMG signal. The general impression was that a shorter residual limb could produce a larger muscle deformation (we asked all subjects to reach the maximum contraction) but longer one could generate more stable SMG signals and the subject felt that the muscle contraction was easier to control. Further studies with more amputee subjects with different features of residual limbs are necessary to confirm these findings. It was also noted that the curve of the transient muscle deformation of the amputee was not so smooth in comparison with the curves of the normal subjects. One important reason is that the subject did not have visual feedback of the phantom wrist extension during the muscle

contraction. Further studies are definitely required to demonstrate the potentials of SMG for the prosthesis control and to investigate effects of many factors that may affect the quality of the SMG signals, such as the residual limb length, muscle quality, surgical procedures, etc.

The results of the normal subjects demonstrated that the ratios between the wrist angle and the percentage deformation obtained using linear regressions were significantly different among the 6 subjects (overall mean 7.2 ± 3.7 deg/%). The result of one subject was dramatically smaller than those of the other subjects. The ratio of this subject (1.2 deg/%) was about 10 times less than the maximum value (12.4 deg/%). It could be visually observed from the dynamic ultrasound images that the muscle of this subject deformed very obviously during the wrist extension. In addition, this subject had the smallest muscle thickness (15.2 mm) among all the normal subjects. The exact reason for this special case was beyond the main topic of this study and thus has not been further investigated. Experiments on more subjects with different age, gender, and physical conditions are required to better understand the main factors which determine the ratio between the joint angle and the muscle deformation.

Ultrasound images can inherently be used to detect the motions of tissues at different locations and different depths as long as their cross-sections can be viewed in the image (*Figure 4*). Therefore, it is possible to obtain SMG signals for different groups of muscles so that the motions of individual joints can be predicted. Since the main purpose of this paper is to demonstrate the feasibility to collect SMG signals from forearm muscles, the motion tracking for different groups of muscles had not been particularly considered during

the image collection. Further experiments are being planned to extract multiple channels of SMG signals. It is well known that it is rather difficult to use EMG signals to differentiate activities of overlapped muscle groups, as the EMG signals of these muscles are combined together when they are collected on the skin surface. This advantage of SMG over EMG should be further verified together with other factors that may affect the collection and extraction of the SMG signals.

In the present study, a portable ultrasound scanner was used to collect the cross-sectional images (B-mode ultrasound, i.e. brightness mode) of the forearm tissues. It is useful for the dynamic assessment of limb tissues using the extracted SMG signals. However, it is not feasible to use it for the control purpose, as the system is too expensive and the ultrasound probe is too large. We have demonstrated that SMG signals could also be obtained using a single element ultrasound transducer and single channel pulse/receiver to obtain one dimensional ultrasound signal (A-mode ultrasound, i.e. amplitude mode). The results will be reported elsewhere. Such a system can be much cheaper and may potentially be installed into the powered prosthesis. Since only one A-mode ultrasound signal could be collected, the obtained SMG signal was sensitive to the location of the ultrasound transducer. To solve this problem, multiple channels of single element transducers have been proposed. Nevertheless, the present study using a B-mode ultrasound scanner allowed us to demonstrate the feasibility to obtain SMG signals from the limb tissues. During the study, we also noted that other factors could also affect the collection of the SMG signals, which are discussed as follow.

In the current experiments, only the wrist extension was performed and other joints were

kept stable. However, different joints may move together in the real situation. It is expected that the SMG signal collected from the forearm tissues might also be affected by the motion or position of the elbow and other joints. Further studies should be followed up to clarify this issue and to study how to reduce the “cross-talk” of the SMG signals among different joints. Multiple channels of SMG can be collected from the muscle groups controlling the corresponding joints so that proper signal processing methods including artificial neural networks [5-8], can be applied to differentiate different types of movements of the joints. In addition, the SMG of the forearm tissues was collected without any load applied on the wrist. In the real situation, the hand may hold some weights during the wrist extension. It has already been demonstrated that the muscle dimension may change during the isometric contraction. Therefore, the SMG signal might be affected when the hand holds certain weights. The factor might be neglected in the case of residual limbs, as no load could be applied on the wrist extensor muscles. However, it should be considered that the residual limb might be compressed by the wall of the prosthesis socket. We found that the amplitude of the SMG signal would be reduced if the tissues were compressed by the ultrasound probe. Further studies are required to quantitatively document the change of SMG induced by the pressure applied on the skin. Moreover, we do not know yet whether the speed of the joint motion would affect the SMG signal or not. The amplitude of the EMG signal may be related to the contraction speed of the muscle [45-47]. Further studies are required to investigate how the speed of the joint motion affects the SMG signals so that the physiological meaning of the SMG signal, i.e. the change of the cross-sectional dimension, could be better understood. Morphological changes as alternative signals for the musculoskeletal control have been reported by a number of groups, but their relationship with the functional outputs of the muscle has not been well addressed. Further studies

towards this direction can help to establish models to investigate the muscle mechanics or neuro-physiological control mechanisms with the SMG signal measured using ultrasound non-invasively.

The relationship between the muscle architecture and its functional capabilities has recently attracted many research efforts [48]. It has been widely reported that the pennation angle of the muscle fibers are highly related to the muscle force and the range of motion [49]. Since the volume of a specific muscle can be assumed constant during muscle contractions [50], the pennation angle is related to the cross-sectional area of the muscle, which in turn is related to the muscle thickness. The change of the muscle thickness is defined as sonomyography, i.e. SMG, in the present study. It should be a research direction to model the relationship between SMG and the muscle force as well as SMG and the range of motion controlled by this muscle. Furthermore, the dynamic change of the pennation angle or muscle cross-sectional area can also be directly obtained from the ultrasound images by improving the ultrasound technique proposed in this study. Therefore, we can have pennation angle SMG or cross-sectional area SMG in addition to muscle deformation SMG. All these indicate that SMG with further investigations may have good potentials for the musculoskeletal assessment besides the control purpose as demonstrated in this study.

In spite of the above factors that need to be further investigated, the present study has already demonstrated that the SMG signal could be reliably collected from the forearm muscles of six normal subjects and three amputee subjects. It was also found that there was a good linear relationship between the wrist extension angle and the percentage deformation of the extensor muscle. The magnitude of the SMG signal collected from the residual limbs

of the amputee subjects were at a similar level to those of the normal subjects. Our preliminary results demonstrated that the SMG signal could be potentially used for the control of prosthesis or other purposes currently involving the EMG signal. Further studies are definitely required to demonstrate the real potentials of this new signal, which is related to the morphological change of the musculoskeletal tissues during contraction. We also expect that the SMG signal might be used together with the EMG signal to provide more comprehensive information for the musculoskeletal assessment and control. The correlation between the SMG and EMG signals should be established with further experiments.

**Acknowledgements**

This work was partially supported by the Research Grants Council of Hong Kong (PolyU 5245/03E) and The Hong Kong Polytechnic University. Miss Grace H.Y. Lo helped in the data collection for two amputee subjects.

**References**

[1] Scott RN and Parker PA. Myoelectric prostheses – state of the art. Journal of Medical Engineering and Technology 1988; 12: 143-51.

[2] Winter DA. Biomechanics and motor control of human movement. 2nd ed, London: Wiley, 1990.

[3] Kenney LPJ, Lisitsa I, Bowker P, Heath GH, and Howard D Dimensional change in muscle as a control signal for powered upper limb prostheses: a pilot study. Med Eng Phys 1999; 21: 589-97.

[4] Aghili F and Haghpanahi M. Use of a pattern recognition technique to control a

multifunctional prosthesis. J Biomed Eng 1995; 42: 504-8.

[5] Hudgins B, Parker PA, Scott RN. A new strategy for multi-function myoelectric control. IEEE Trans Biomed Eng 1993; 40: 82-94.

[6] Chan FHY, Yang YS, Lam FK, Zhang YT, and Parker PA. Fuzzy EMG classification for prosthesis control. IEEE Trans Rehab Eng 2000; 8: 305-11.

[7] Micera S, Sabatini AM, Dario P, and Rossi B. A hybrid approach to EMG pattern analysis for classification of arm movements using statistical and fuzzy techniques. Med Eng Phys 2001; 21: 303-311.

[8] Englehart K and Hudgins B. A robust, real-time control scheme for multifunction myoelectric control. IEEE Trans Biomed Eng 2003; 50: 848-854.

[9] Heasman JM, Scott TRD, Kirkup L, Flynn RY, Vare VA, and Gschwind CR. Control of a hand grasp neuoprosthesis using an electroencephalogram-triggered switch: demonstration of improvements in performance using wavepacket analysis. Med Biol Eng Compt 2002; 40: 588-593.

[10] Nicolelis MAL. Actions from thoughts. Nature, 409: 403-407, 2001.

[11] Taylor DM, Tillery SIH, and Schwartz AB. Direct cortical control of 3D neuroprosthetic device. Science 2002; 296: 1829-1832.

[12] Wolpaw JR, Birbaumer N, McFarland DJ, Pfurtscheller G, and Vaughan TM. Brain-computer interfaces for communication and control. Clin Neurophysiol 2002; 113: 767-791.

[13] Qin L. Morphological studies on prevention of immobilization atrophy of skeletal muscle by electrical stimulation. PhD thesis, German Sports University, Cologne, F.R.G., March, 1992

[14] Qin L, Appell H-J, Chan KM, Maffuli N. Electrical stimulation prevents immobilization atrophy in skeletal muscle of rabbits. Arch Phys Med Rehab 1997; 78:512-517.

[15] Oster G. Muscle sound. Sci Am 1984; 250: 108-114.

[16] Bolton CF, Parkers A, Thompson TR, Clark MR, and Sterne CJ. Recording sound from human skeletal muscle: Technical and physiological aspects. Muscle Nerve, 1989; 12: 126-134.

[17] Orizio C. Muscle sound: bases for the introduction of a mechnomoygraphic signal in

muscle studies. Crit Rev Biomed Eng 1993; 21: 201-243.

[18] Yoshitake Y, Shinohara M, Ue H, Moritani T. Characteristics of surface mechanomyogram are dependent on development of fusion of motor units in humans. J Appl Phys 2002; 93: 1744-1752.

[19] Weir RF, Heckathorne CW, and Childress DS. Cineplasty as a Control Input for Externally-Powered Prosthetic Components, J Rehab Res Dev 2001; 38: 357-363.

[20] Childress DS. Tunnel Cineplasty. J Rehab Res Dev 2002; 39(suppl.): 9-10.

[21] Wilms E and Nader L. Der Technik der Vaduzer Hand Orthopaedie Technik 1951; 2: 7.

[22] Almstrom C and Kadefors R. Methods for transducing skin movements in the control of assistive devices. In Proceedings of 3rd International Conference on Medical Physics, Goteborg, Sweden, 1972; 33: 2.

[23] Rafolt A and Gallasch E. Surface myomechanical responses recorded on a scanner galvanometer. Med Biol Eng Compt 2002; 40: 594-9.

[24] Abboudi RL, Glass CA, Newby NA, Flint JA, and Craelius W. A biomimetic controller for a multifinger prosthesis. IEEE Trans Rehab Eng 1999; 7: 121-129.

[25] Curcie DJ, Flint JA, and Craelius W. Biomimetic finger control by filtering of distributed forelimb pressures. IEEE Trans Neural Sys Rehab Eng 2001; 9: 69-75.

[26] Craelius W. The bionic man: restoring mobility. Science 2002; 295: 1018-21.

[27] Van Holsbeeck MT and Introcaso JH. Sonography of muscle. In: Van Holsbeek MT and Introcaso JH (Eds) Musculoskeletal Ultrasound, 2nd. Mosby, St. Louis, 2001, p. 23-75.

[28] Nakamichi K and Tachibana S. Restricted motion of the median nerve in carpal tunnel syndrome. J Hand Surg 1995; 20: 460-4.

[29] Hough AD, Moore AP, and Jones MP. Measuring longitudinal nerve motion using ultrasonography. Manual Ther 2000; 5: 173-80.

[30] Bertrand M Meunier J, Doucet M, and Ferland G. Ultrasonic biomechanical strain gauge based on speckle tracking. Proc IEEE Ultrason Symp, 1989, p. 859-63.

[31] Meunier J and Bertrand M. Echographic image mean gray level changes with tissue dynamics: A system-based model study. IEEE Trans Biomed Eng 1995; 42: 403-10.

[32] Fukunaga T, Ito M, Ichinose Y, Kuno S, Kawakami Y, and Fukashiro S. Tendinous movement of human muscle during voluntary contractions determined by real-time

ultrasonography. J Appl Physiol 1996; 81:1430-1433.
[33] Ito M, Akima H, and Fukunaga T. In vivo moment arm determination using B-mode ultrasonography. J Biomech 2002; 33: 215-218.
[34] Maganaris CN. Tensile properties of in vivo human tendinous tissue. J Biomech 2002; 35: 1019-1027.
[35] Ophir J, Alam SK, Garra B, Kallel F, Konofagou E, Krouskop T, and Varghese T. Elastography: ultrasonic estimation and imaging of the elastic properties of tissues. Proc Instn Mech Engrs 1999; 213 (Part H): 203-33.
[36] Gao L, Parker KJ, Lerner RM, Levinson SF. Imaging of the elastic properties of tissue - A review. Ultrasound Med Biol 1996; 22: 959-977.
[37] Lovelace AM, Bhagat PK, Wu VC. Apparatus for determining changes in limb volume. US Patent No. 4,383,533, 1983.
[38] Manthey JK. Method and apparatus for stimulation of posture. US Patent No. 5,433,201, 1995.
[39] Hodges PW, Pengel LHM, Herbert RD, and Gandevia SC. Measurement of muscle contraction with ultrasound imaging. Muscle and Nerve 27: 682-692, 2003.
[40] Convey P and Murray KD. Ultrasound study of the motion of the residual femur within a trans-femoral socket during gait. Prosthet Orthot Int, 24: 226-232, 2000.
[41] McMeeken JM, Beith ID, Newham DJ. The relationship between EMG and change in thickness of transversus abdominis. Clin Biomech 2004; 19: 337-342.
[42] Platt RS, Kieser TM, and Easton PA. Eliminating ultrasonic interference from respiratory muscle EMG. Respir Physiol 1998; 113: 203-213.
[43] Journee HL, et al. Ultrasound myography – application in nerve-conduction velocity assessment and muscle cooling. Ultrasound Med Biol 1993; 19: 561-566.
[44] Huang QH, Zheng YP, Lu MH, and Chi ZR. Development of a portable 3D ultrasound imaging system for musculoskeletal tissues. Ultrasonics 2005; 43: 153-163.
[45] Cramer JT, Housh TJ, Johnson GO, Ebersole KT, Perry SR, Bull AJ. Mechanomyographic amplitude and mean power output during maximal, concentric, isokinetic muscle actions. Muscle Nerve 2000; 23: 1826-1831.
[46] Rothstein JM, Delitto A, Sinacore DR, Rose SJ. Electro-myographic, peak torque, and power relationships during isokinetic movement. Phys Ther 1983; 63: 926-933.

[47] Barnes WS. The relationship of motor-unit activation to isokinetic muscular-contraction at different contractile velocities. Phys Ther 1980; 60: 1152-1158.
[48] Van der Linden BJJJ, Koopman HFJM, Grootenboer HJ, and Huijing PA. Modelling functional effects of muscle geometry. J Electromyography and Kinesiology 1998; 8: 101-109.
[49] Scoh SH, Winter DA. A comparison of three muscle pennation assumptions and their effect on isometric and isotonic force. J Biomechanics 1991; 24: 163-167.
[50] Kardel T. Niels Stensens geometrical theory of muscle contractions (1667): a reappraisal. J Biomechanics 1990; 23: 953-965.

**Figure Captions**

**Figure 1.** Setup for the simultaneous collection of the ultrasound images using the portable ultrasound scanner and the motion data using the motion analysis system.

**Figure 2.** Placement of the reflective markers and the ultrasound probe on the forearm. Ultrasound coupling gel was applied between the ultrasound probe and the skin surface to couple the ultrasound signal into the tissue.

**Figure 3.** Program interface for the image and signal processing for the muscle boundaries tracking and deformation calculation.

**Figure 4.** Tracking blocks added on the ultrasound image of cross-sectional view of the forearm for measuring the muscle deformation. The tracking blocks were set to cover the upper and lower boundary of the extensor carpi radialis.

**Figure 5.** Setup for collecting ultrasound images from the residual forearm of the amputee (subject #1). The metronome was used to guide the subject to contract and relax the residual muscle. Ultrasound coupling gel was applied between the ultrasound probe and the skin surface to couple the ultrasound signal into the tissue.

**Figure 6.** Transient wrist angle and muscle deformation of a typical trial with three cycles of wrist extension on subject F.

**Figure 7.** The plot of the wrist extension angle versus the percentage muscle deformation of the typical trial shown in Figure 6. The linear regression is used to represent the relationship between the wrist extension angle and the percentage muscle deformation.

**Figure 8.** The ratio of the wrist extension angle and the percentage muscle deformation of the six normal subjects (A-F) tested in this study. The error bar represents the standard deviation of the results of the three trials for each subject. The last bar (mean) represents the overall mean and standard deviation of the results of the six normal subjects.

**Figure 9.** (a) A typical cross-sectional ultrasound image obtained from the residual forearm of the amputee subject #1; (b) Transient muscle deformation of the amputee subject during the three cycles of the muscle contraction of the residual forearm.

**Figure 10**. Experiments for the amputee subject #2. (a) The setup for the measurement; (b) A typical cross-sectional ultrasound image; (c) Transient muscle deformation of the residual arm during the three cycles of the muscle contraction.

**Figure 11**. Experiments for the amputee subject #3. (a) The setup for the measurement; (b) A typical cross-sectional ultrasound image; (c) Transient muscle deformation of the residual arm during the three cycles of the muscle contraction (the middle one was not very successful).

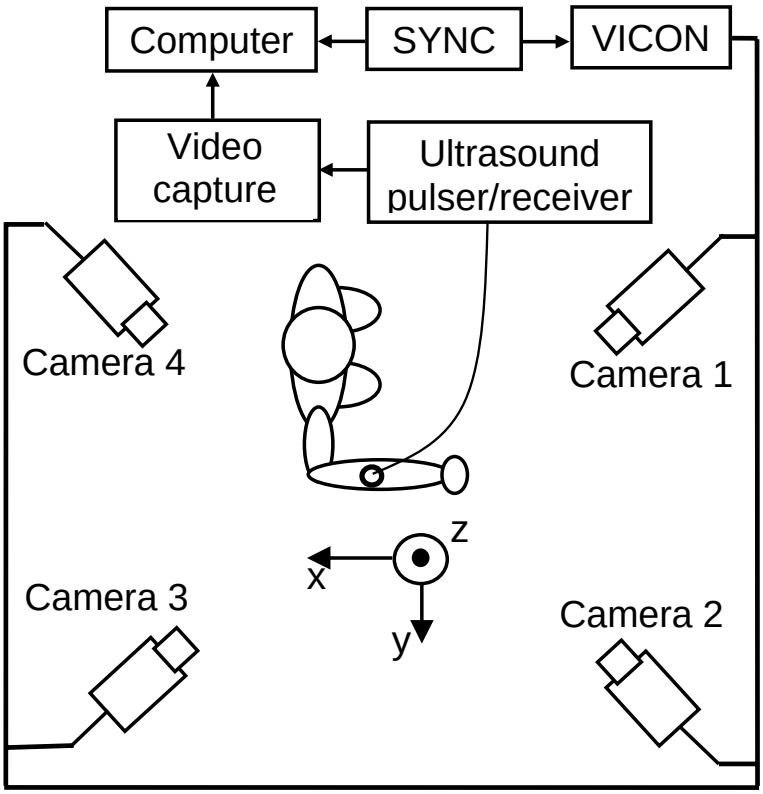
Computer
SYNC
VICON
Video capture
Ultrasound pulser/receiver
Camera 4
Camera 1
Camera 3
Camera 2
z
x
y

1

2 Figure 1.

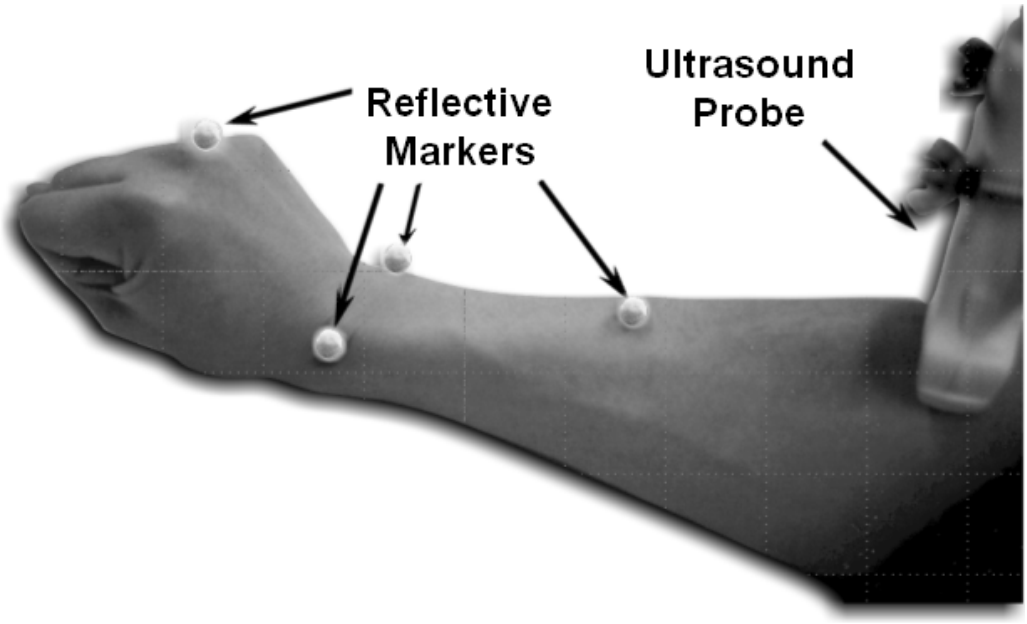


1

2 Figure 2.

3

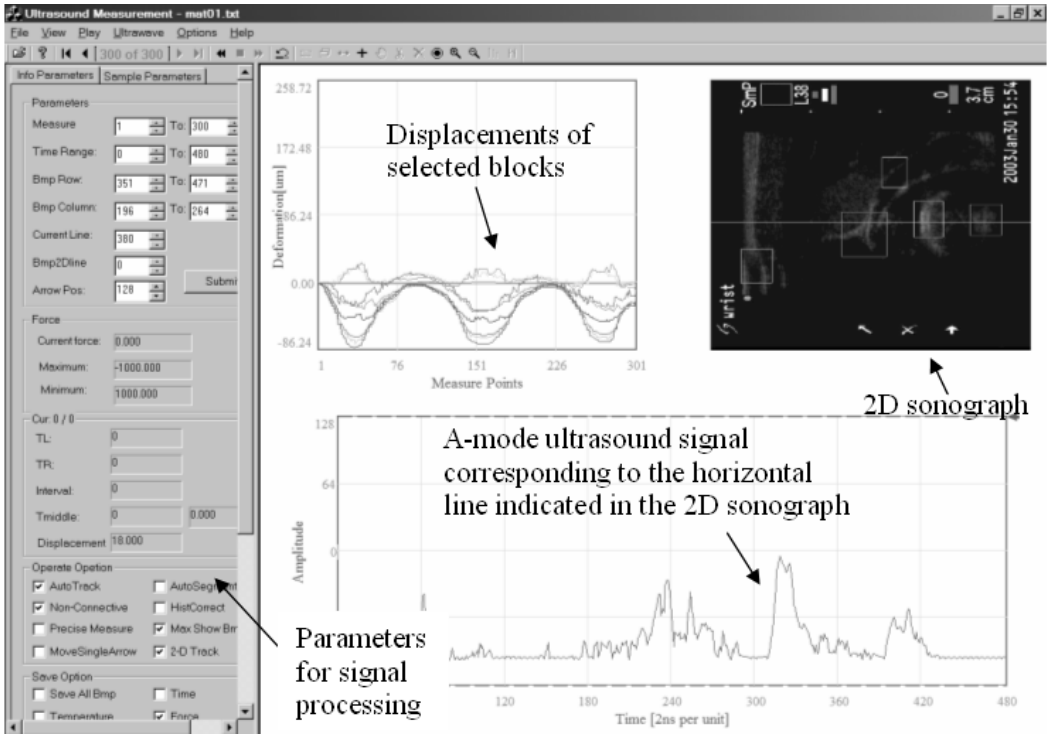
Ultrasound Measurement - mst01.txt
Displacements of selected blocks
Measure Points
2D sonograph
A-mode ultrasound signal corresponding to the horizontal line indicated in the 2D sonograph
Parameters for signal processing
Time [2ns per unit]

Figure 3.

1

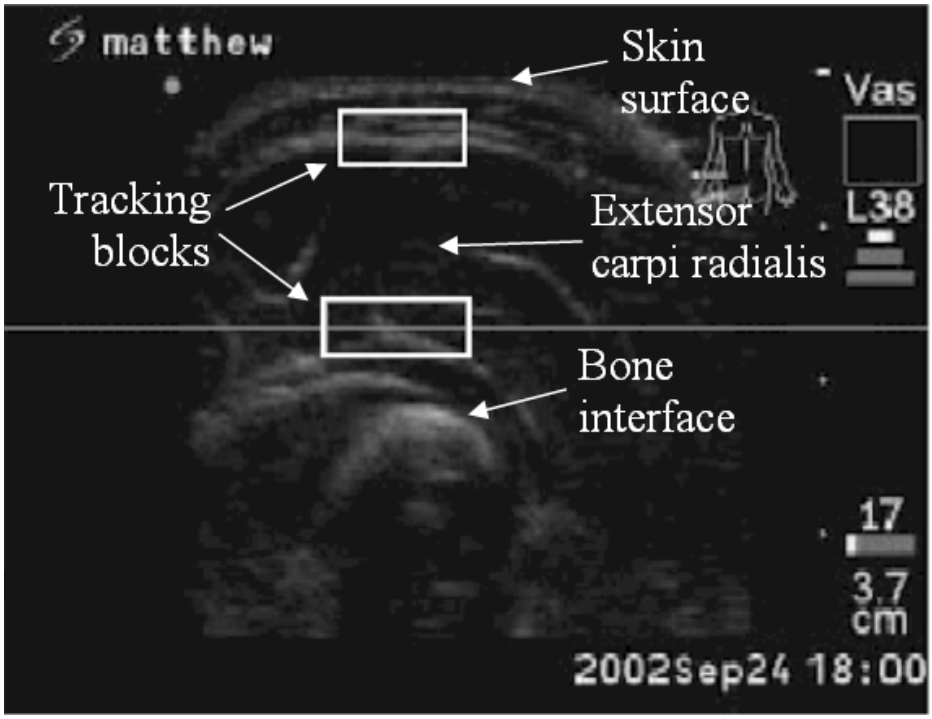


2

3

4 Figure 4.

5

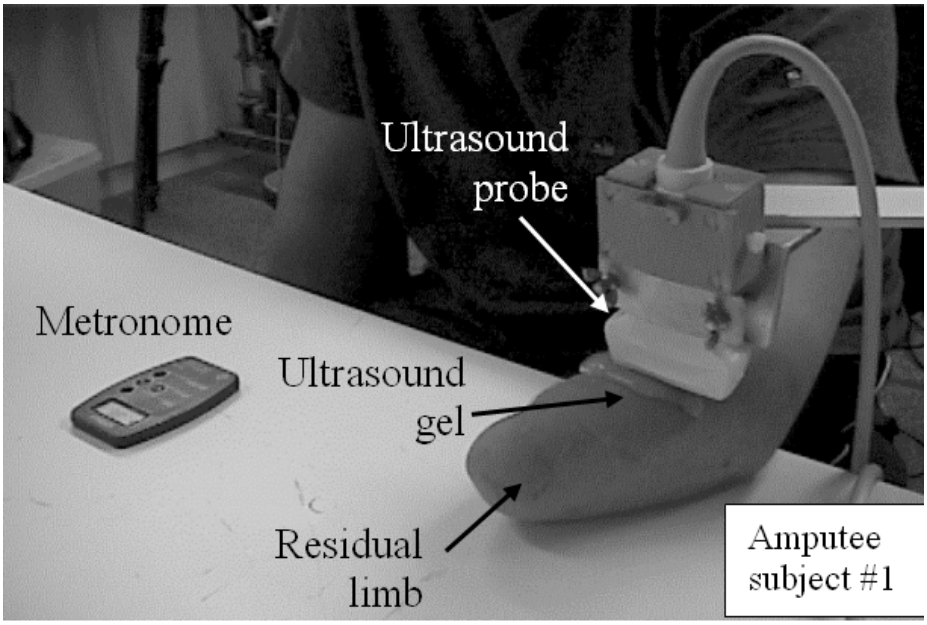
Ultrasound
probe
Metronome
Ultrasound
gel
Residual
limb
Amputee
subject #1

Figure 5.

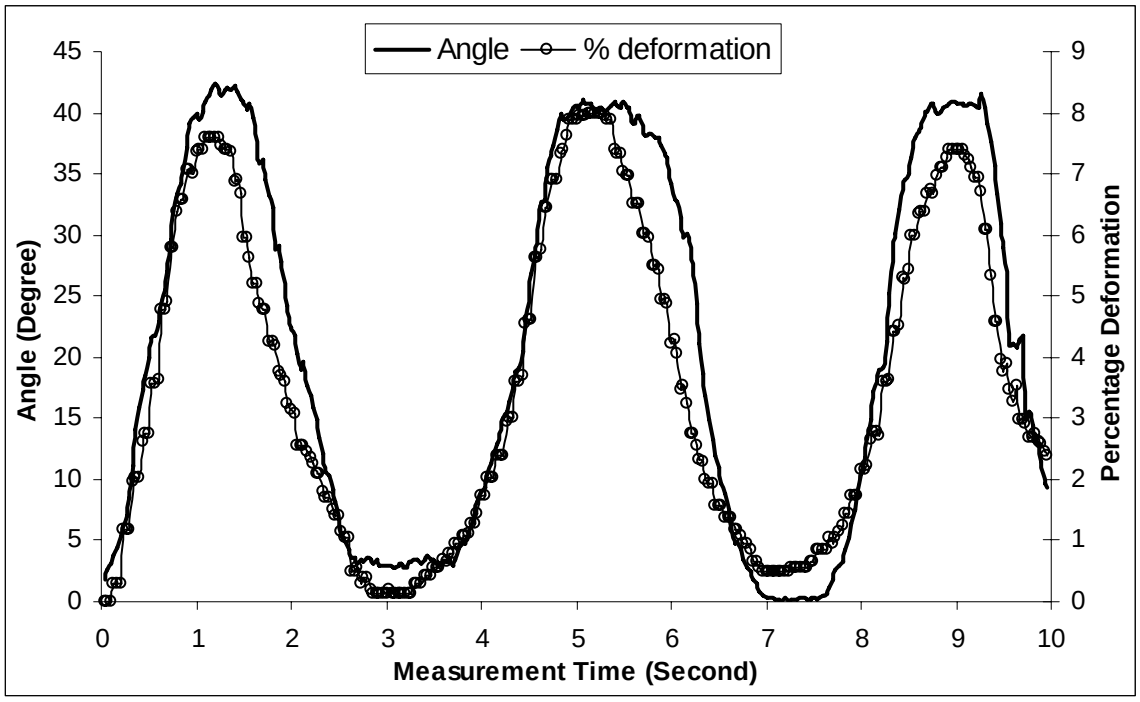
Angle
% deformation
Angle (Degree)
Percentage Deformation
Measurement Time (Second)
0
5
10
15
20
25
30
35
40
45
0
1
2
3
4
5
6
7
8
9
0
1
2
3
4
5
6
7
8
9
10

Figure 6.

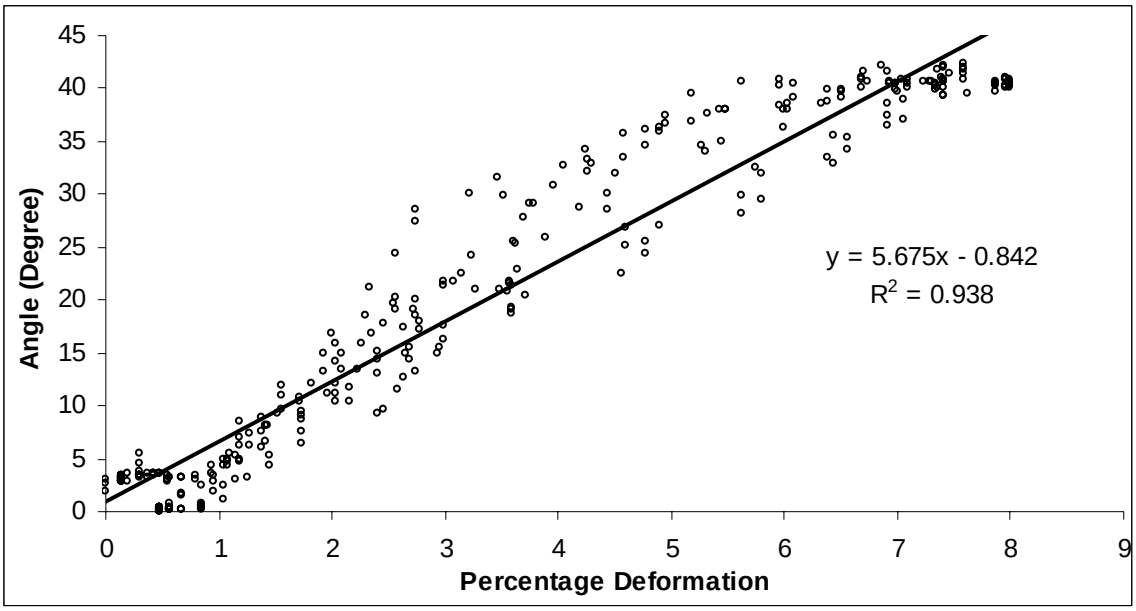
Angle (Degree)
Percentage Deformation
y = 5.675x - 0.842
R2 = 0.938
0
5
10
15
20
25
30
35
40
45
0
1
2
3
4
5
6
7
8
9

Figure 7.

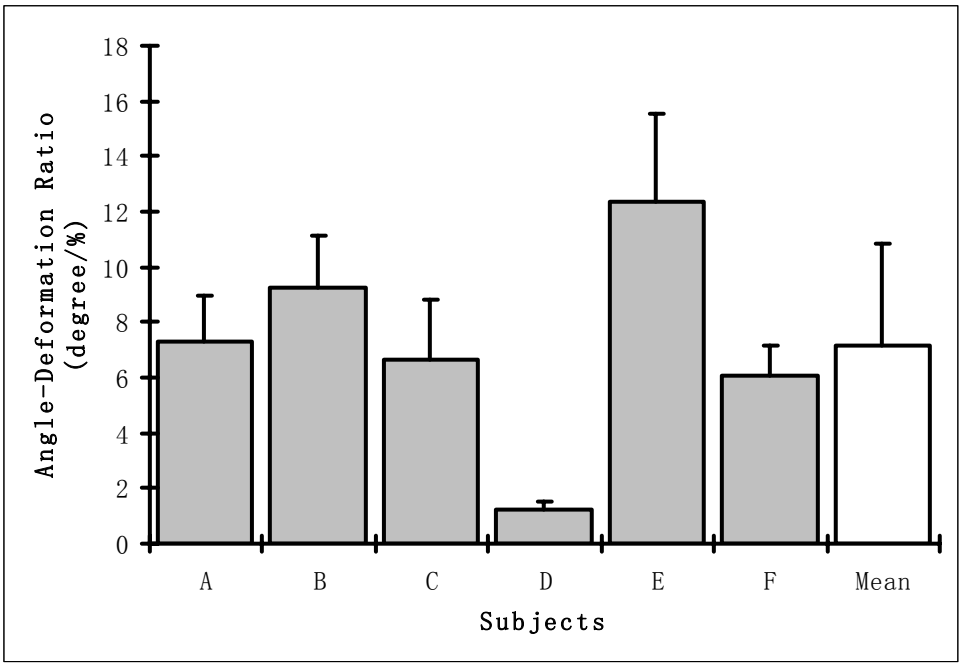
Angle-Deformation Ratio
(degree/%)
18
16
14
12
10
8
6
4
2
0
A
B
C
D
E
F
Mean
Subjects

Figure 8.

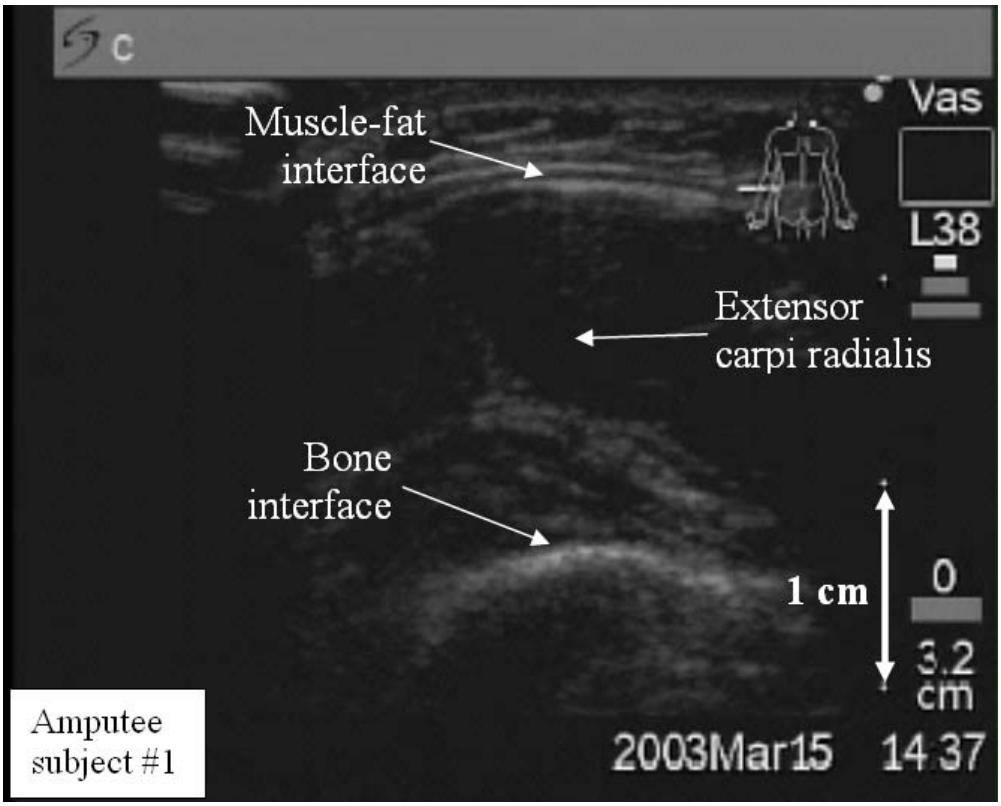
Muscle-fat
interface
Vas
L38
Extensor
carpi radialis
Bone
interface
1 cm
0
3.2
cm
Amputee
subject #1
2003Mar15 14:37

(a)

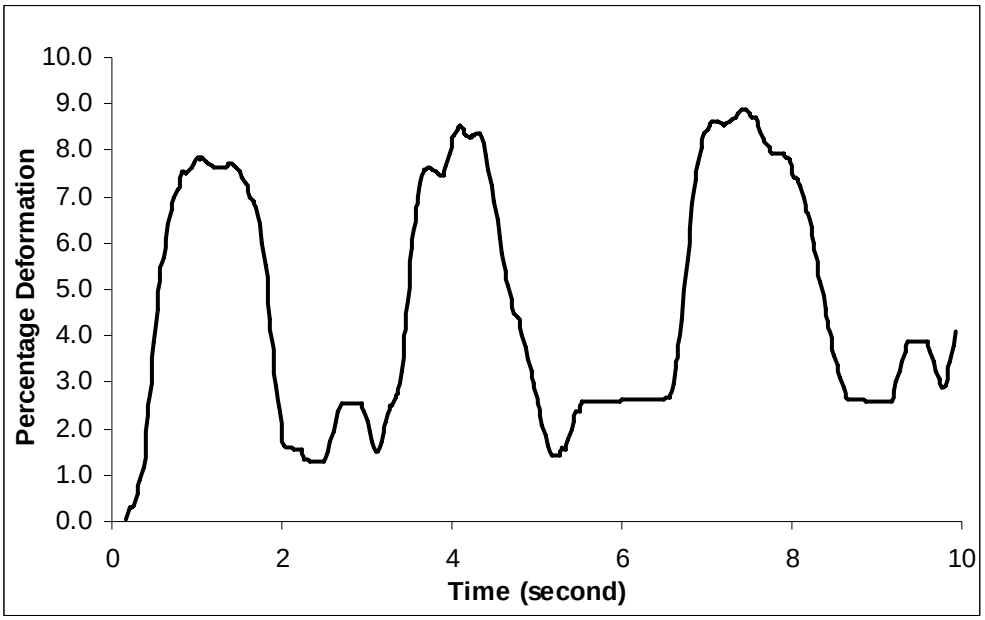
Percentage Deformation
10.0
9.0
8.0
7.0
6.0
5.0
4.0
3.0
2.0
1.0
0.0
0
2
4
6
8
10
Time (second)

(b)

Figure 9.

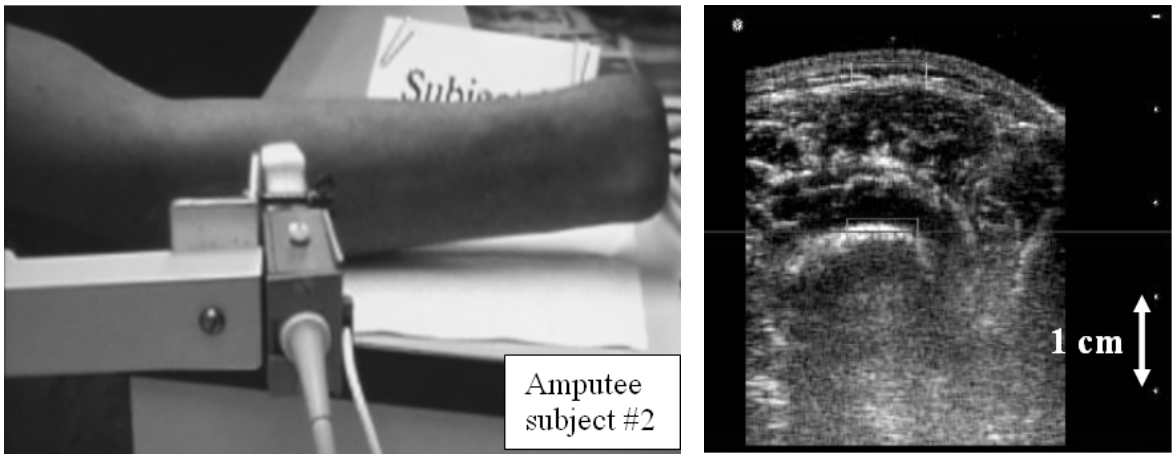


(a) (b)

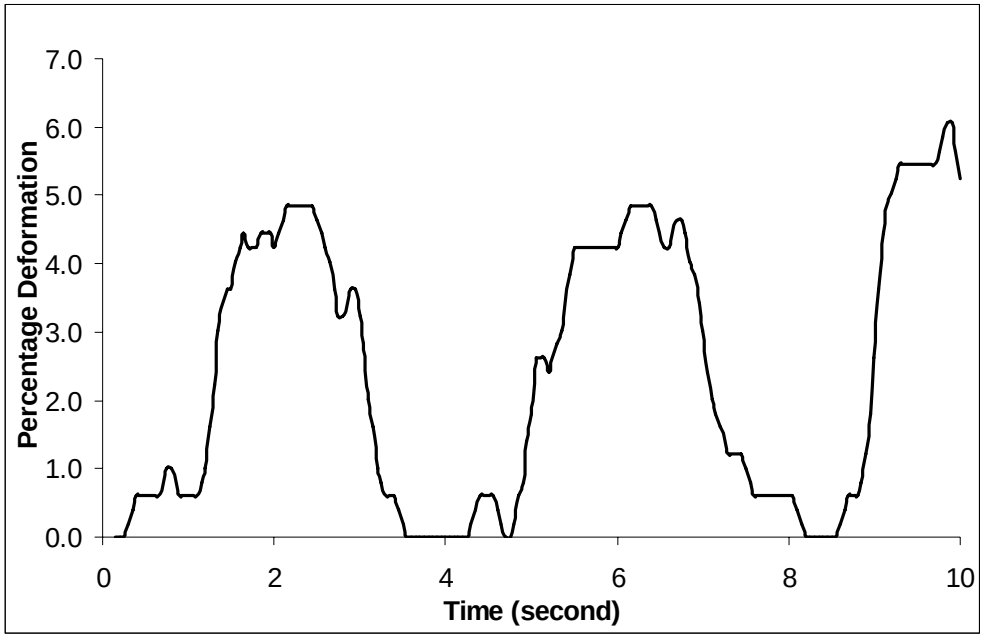


(c)

Figure 10.

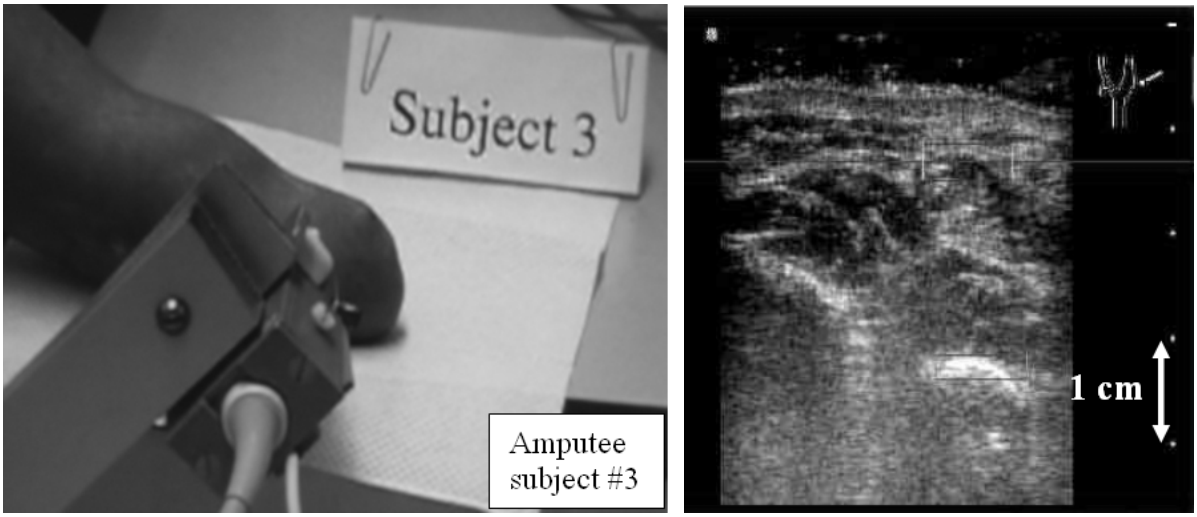


(a) (b)

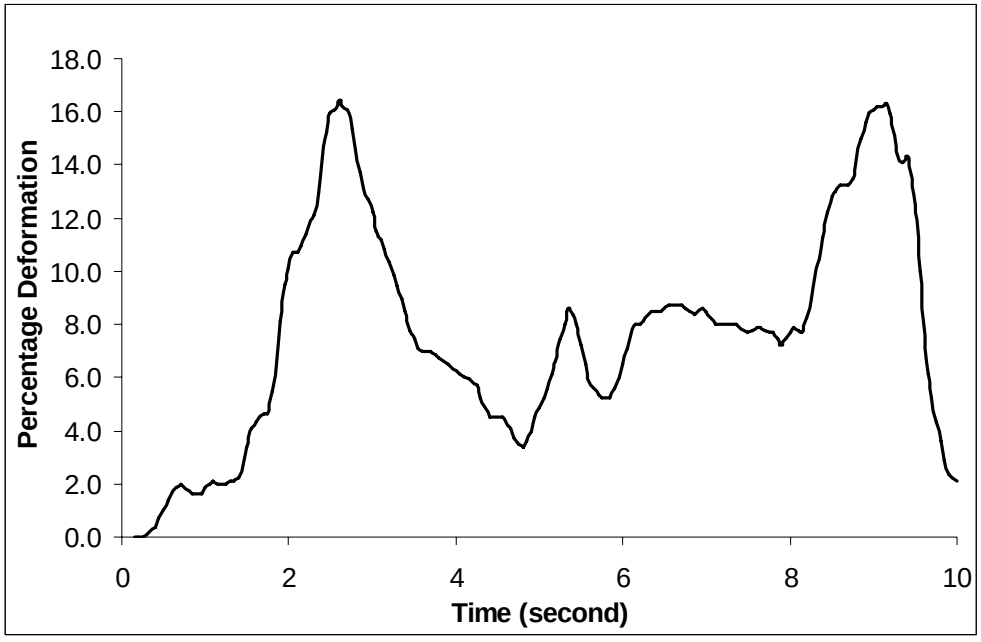


(c)

Figure 11.

1 Table 1. Demographic information of the three amputee subjects.

| | Subject #1 | Subject #2 | Subject #3 |
|---|---|---|---|
| Age (years) | 38 | 42 | 43 |
| Gender | Male | Male | Male |
| Years of amputation | 11 | 24 | 21 |
| Length of residual forearm | ~50% | ~90% | ~30% |
| Prosthesis being used | Powered prosthesis with myo-control | Body-powered prosthesis | Body-powered prosthesis |

2

3